## Supplemental Figures

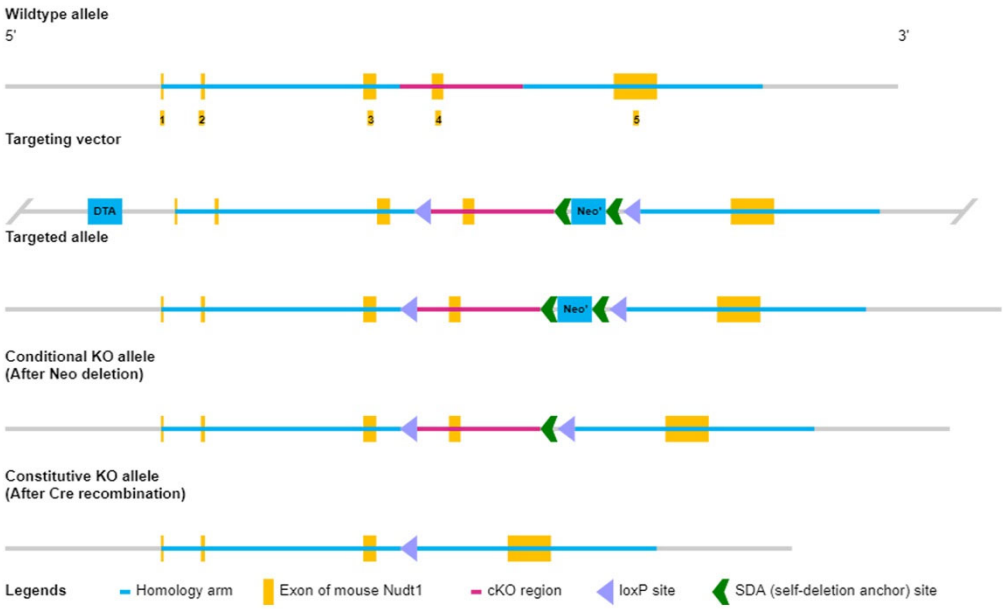


**Figure S1.** Schematic graph of the construction of megakaryocyte/platelet specific MTH1 knockout mice.

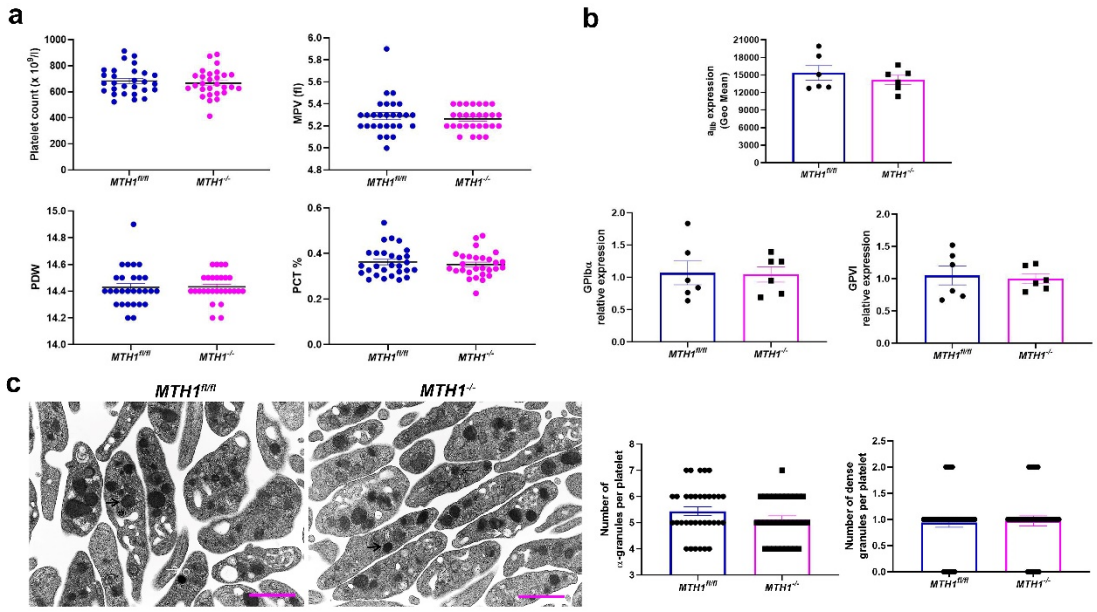


**Figure S2. Platelet count, surface receptors expression and ultrastructure. (a)** Platelet count, mean platelet volume (MPV), platelet distribution width (PDW), plateletcrit (PCT) detected by an automatic blood analyzer (mean± SEM, n=28 independent animals). **(b)** Surface expression of αIIbβ3 (measured by flow cytometry using FITC-conjugated anti-mouse αIIb antibody) ($p$ = 0.4502) GPIbα ($p$ = 0.9136) and GPVI ($p$ = 0.7556) by quantitative real-time PCR (mean ± SEM, n = 6 independent experiments) (two-tailed unpaired student t-test). **(c)** Platelet ultrastructure (α-granules and dense granules) by electron microscopy. Scale bar: 1.0 µm (x 30,000 magnification). Black arrow: α-granule; white arrow: dense granule. The number of α-granules and dense granules was counted in 35 platelets (mean ± SEM, n=35) (two-tailed Mann-Whitney test).

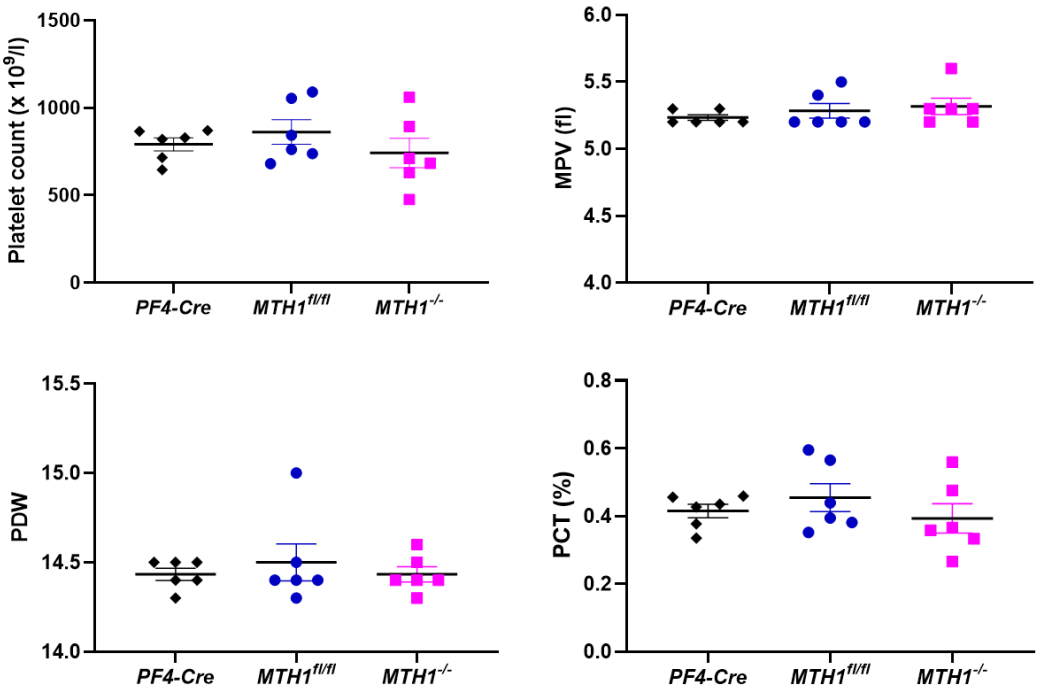


**Figure S3. Platelet parameters in PF4-Cre, MTH1$^{fl/fl}$ and MTH1$^{-/-}$ mice.** Blood was isolated from *PF4-Cre*, *MTH1$^{fl/fl}$* and *MTH1$^{-/-}$* mice to measure platelet count, MPV, PDW and PCT by an automatic blood analyzer (mean ± SEM, n=6 independent animals).

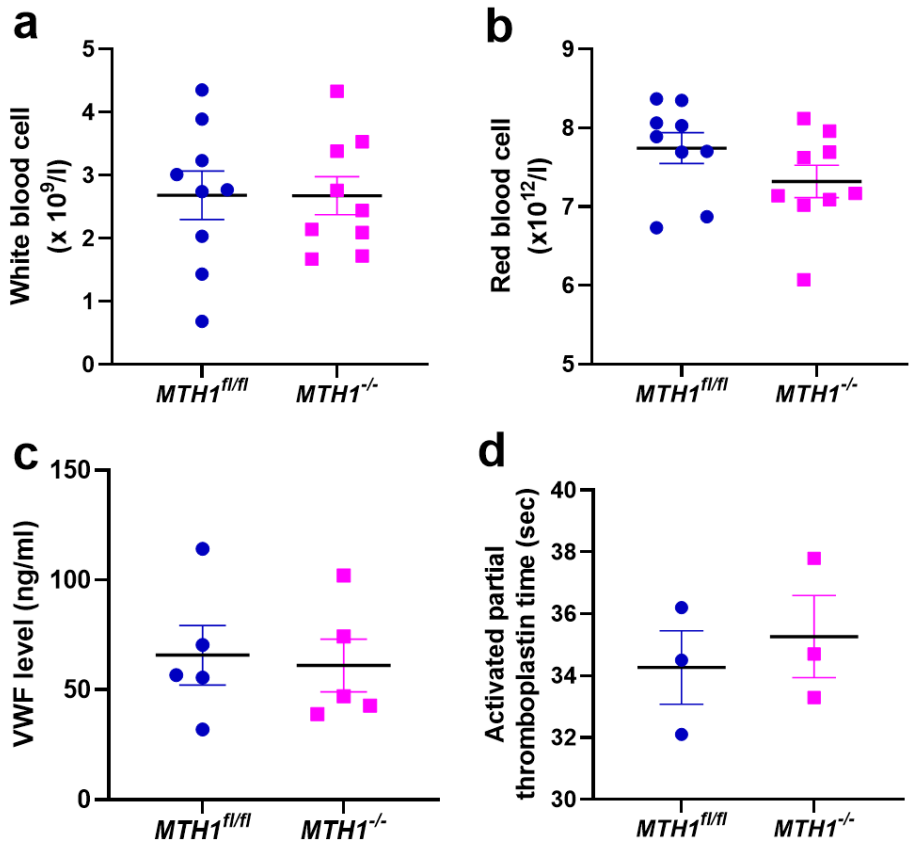


**Figure S4. The number of blood cells, VWF level and coagulation activity.** Blood was isolated from *MTH1*$^{fl/fl}$ or *MTH1*$^{-/-}$ mice to measure the number of white blood cell (mean ± SEM, n = 9 independent animals) **(a)** and red blood cell (mean ± SEM, n = 9 independent animals) **(b)** by an automatic blood analyzer. In addition, plasma was obtained to detect VWF level (mean ± SEM, n = 5 independent animals) **(c)** by ELISA and the activated partial thromboplastin time (mean ± SEM, n = 3 independent animals) **(d)** on an automated coagulation analyzer.

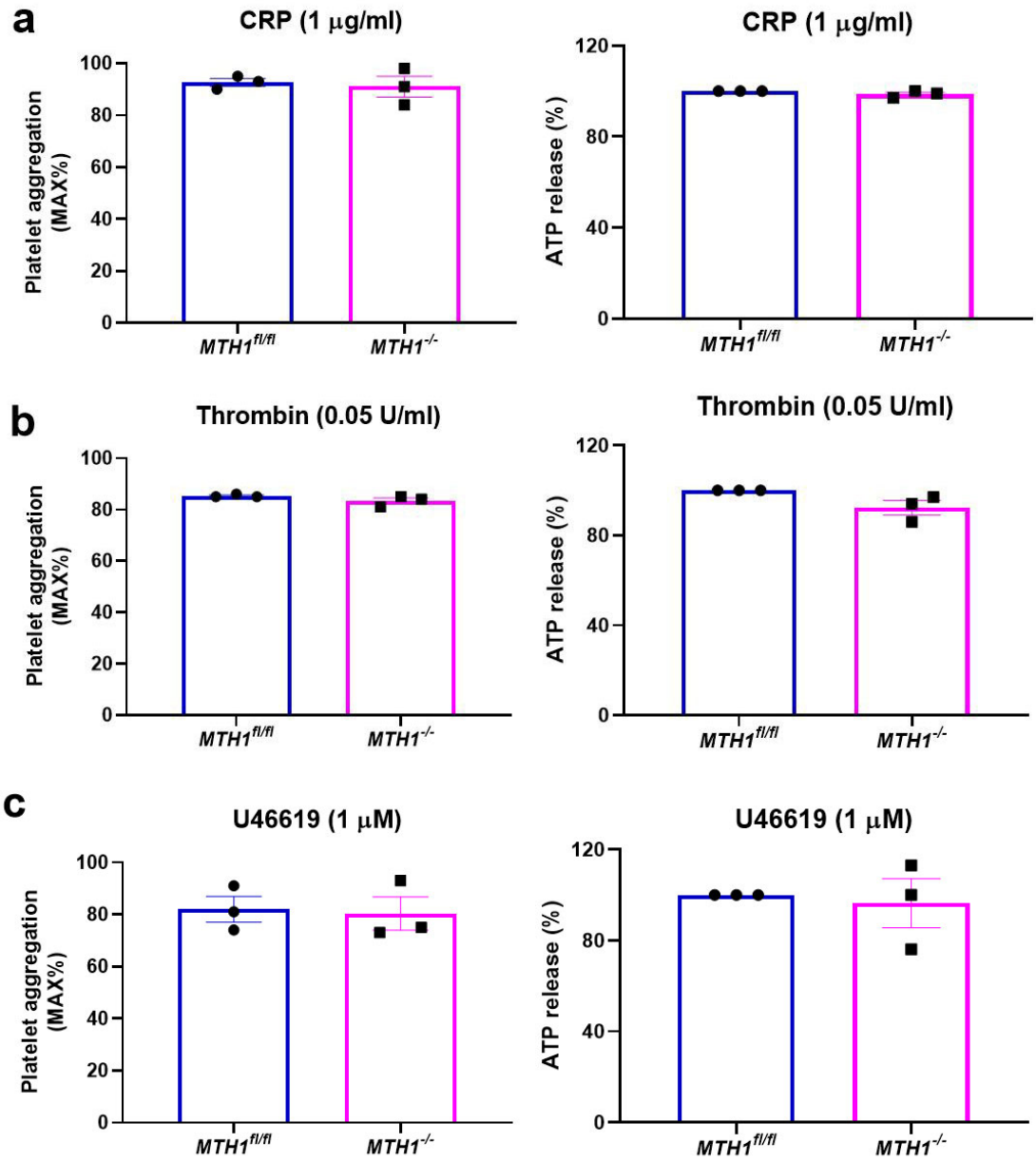


**Figure S5. Platelet aggregation and ATP release.** Washed platelets from *MTH1*$^{fl/fl}$ or *MTH1*$^{-/-}$ mice were stimulated with CRP (a), thrombin (b) or U46619 (c) to measure platelet aggregation and ATP release. Data were shown as mean ± SEM (n = 3 independent experiments).

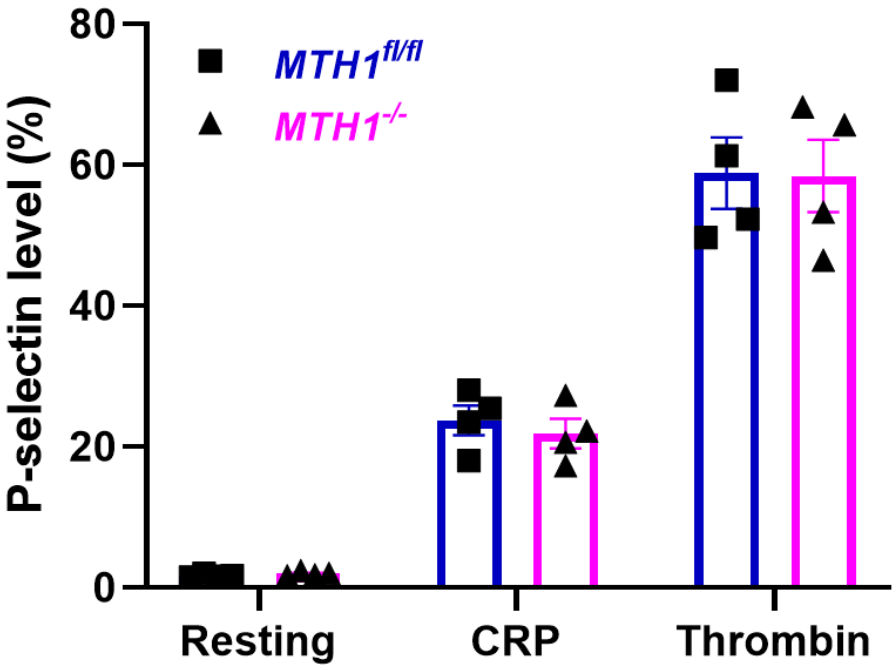


**Figure S6. Platelet P-selectin expression.** Washed platelets were stimulated with CRP (0.5 μg/ml) or thrombin (0.01 U/ml) followed by measuring P-selectin expression by flow cytometry. Data were shown as mean ± SEM (n = 4).

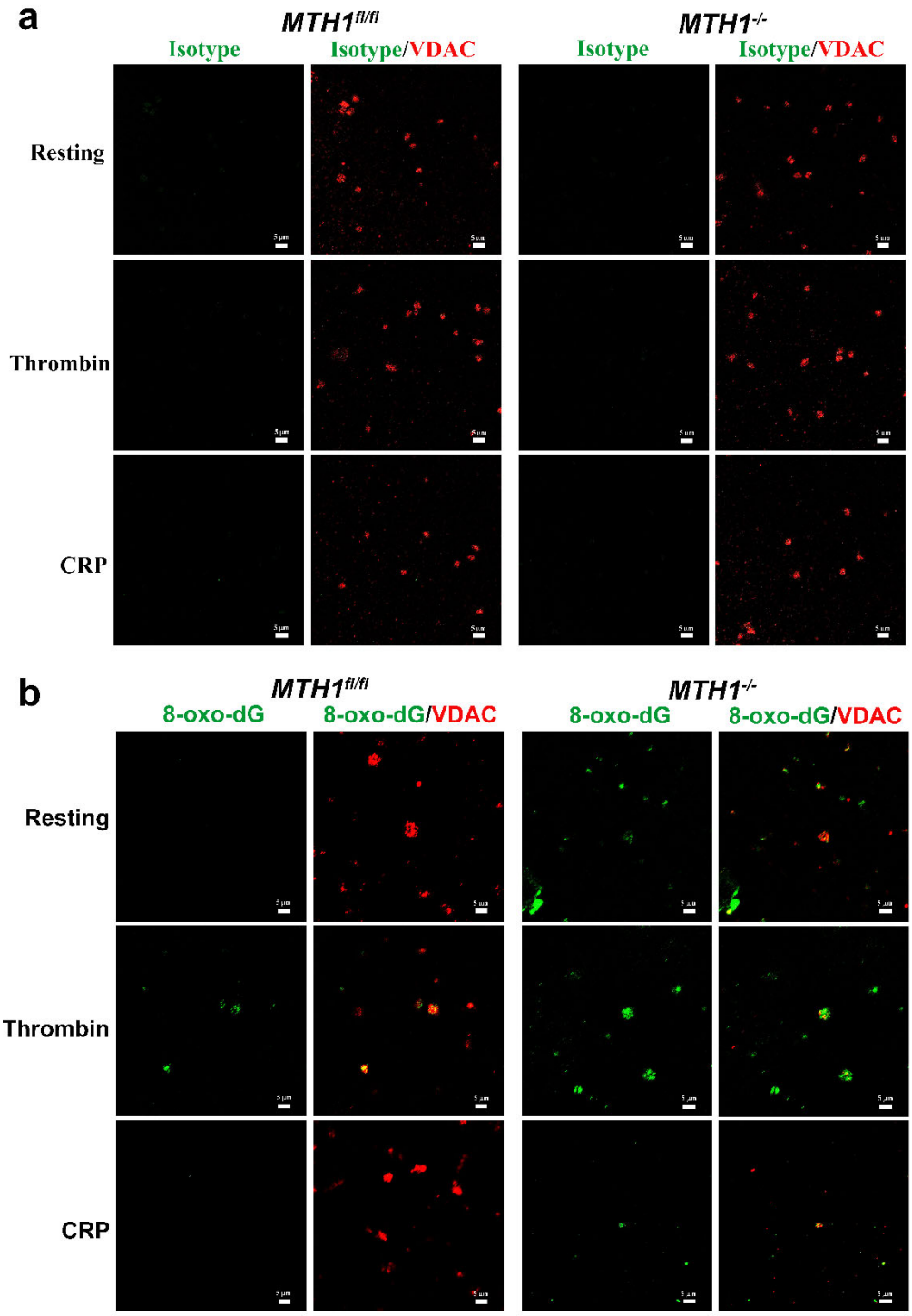


**Figure S7. Accumulation of 8-OHdG in mitochondria.** Mouse platelets were fixed and permeabilized followed by incubation with antibodies against isotype control antibody IgG **(a)**, VDAC or 8-OHdG **(b)** and then with subsequent fluorescence-labelled secondary antibodies. Then, platelets were mounted with Vectashield and staining was visualized under a confocal microscopy. The representative image was shown from 3 independent isolated platelets (n=3). Scale bar = 5 µm.

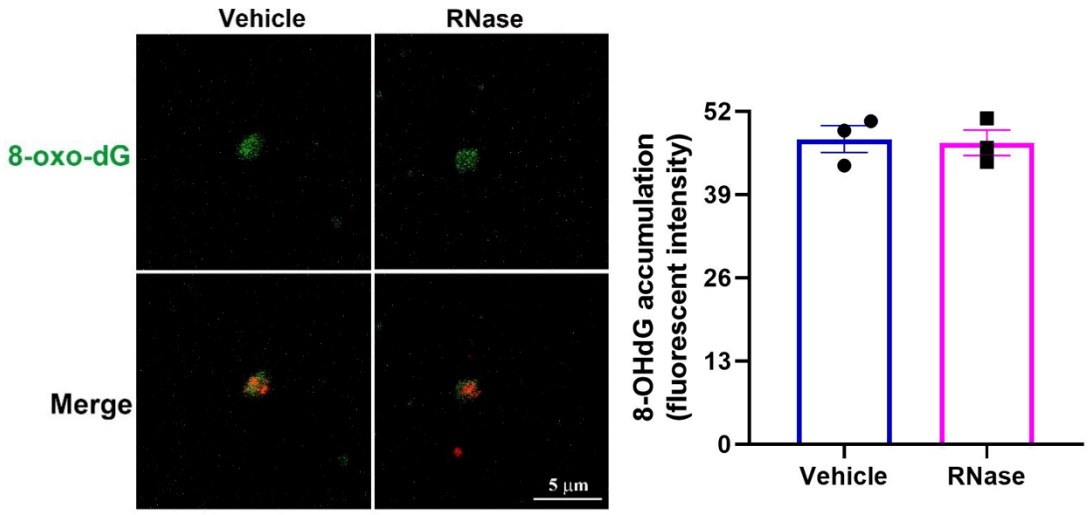


**Figure S8. 8-oxo-dG staining in mouse platelets.** Platelets isolated from *MTH1*$^{-/-}$ mice and stimulated with thrombin (1 U/ml) for 3 min followed by treatment with RNase A (0.02 mg/ml) for 30 minutes at 37°C. After that, platelets were stained with antibodies against with 8-oxo-dG or VDAC and the subsequent with fluorescence-labelled secondary antibodies. Then, the staining was visualized under a confocal microscopy. Representative results from three independent experiments were shown (mean ± SEM, n=3 independent experiments).

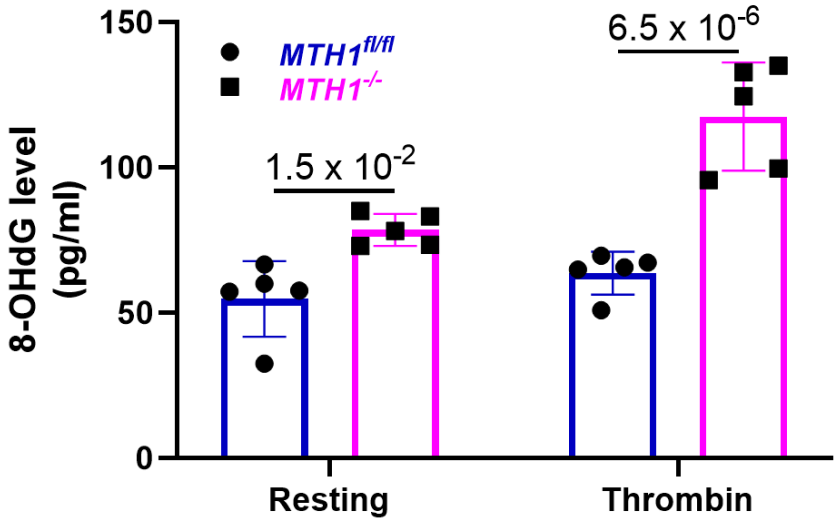


**Figure S9. 8-oxo-dG level in platelets.** Platelets isolated from *MTH1*$^{fl/fl}$ or *MTH1*$^{-/-}$ mice were stimulated with thrombin (1 U/ml) for 3 min to measure the level of 8-oxo-dG by ELISA. Data were shown as mean ± SD (n=5) and assessed by two-way ANOVA with Sidak multiple comparisons test.

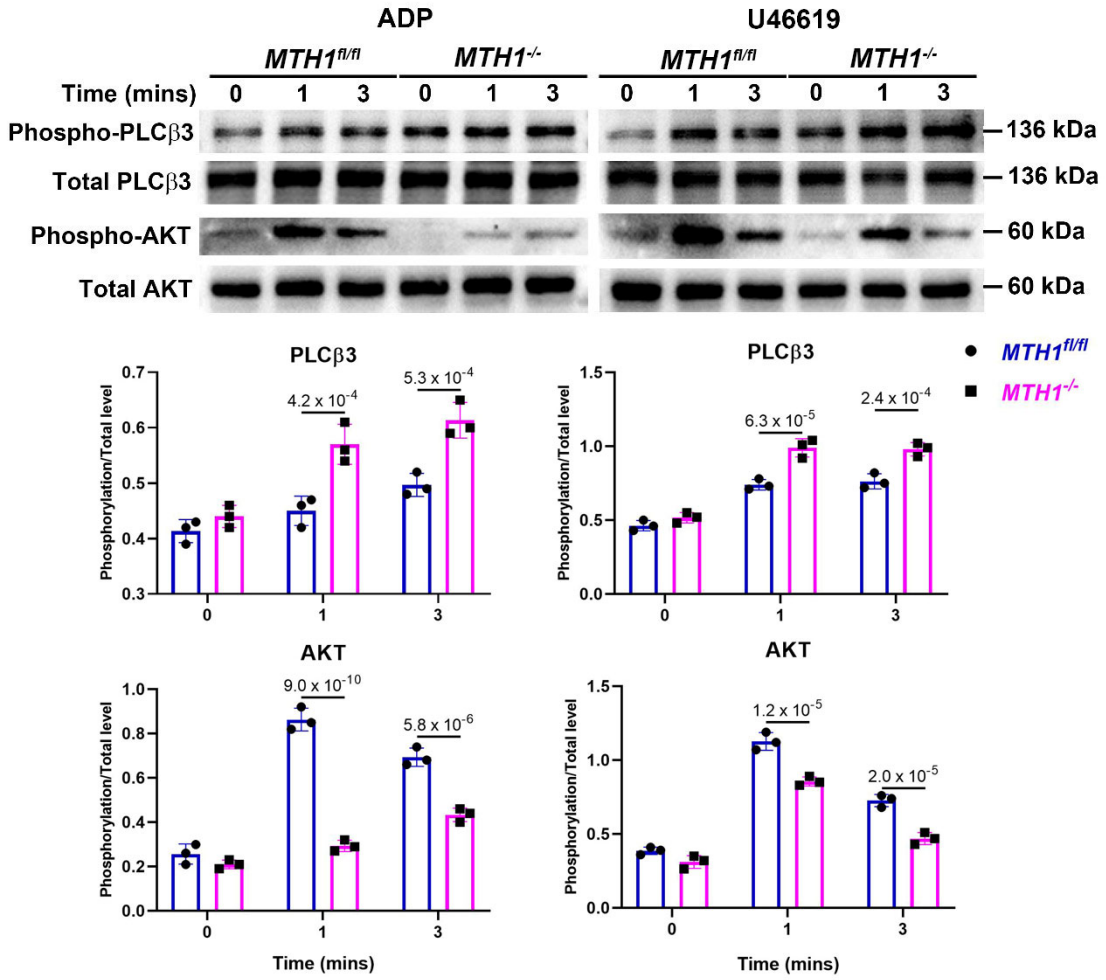


**Figure S10. The phosphorylation level of PLCβ3 and AKT.** *MTH1*$^{fl/fl}$ or *MTH1*$^{-/-}$ platelets were treated with ADP (10 μM) or U46619 (1 μM) for the indicated time points and then the phosphorylation level of PLCβ3 (Ser1105) and AKT (Ser473) was measured. The data were quantified based on three independent experiments (mean ± SD, n = 3, two-way ANOVA with Sidak multiple comparisons test).

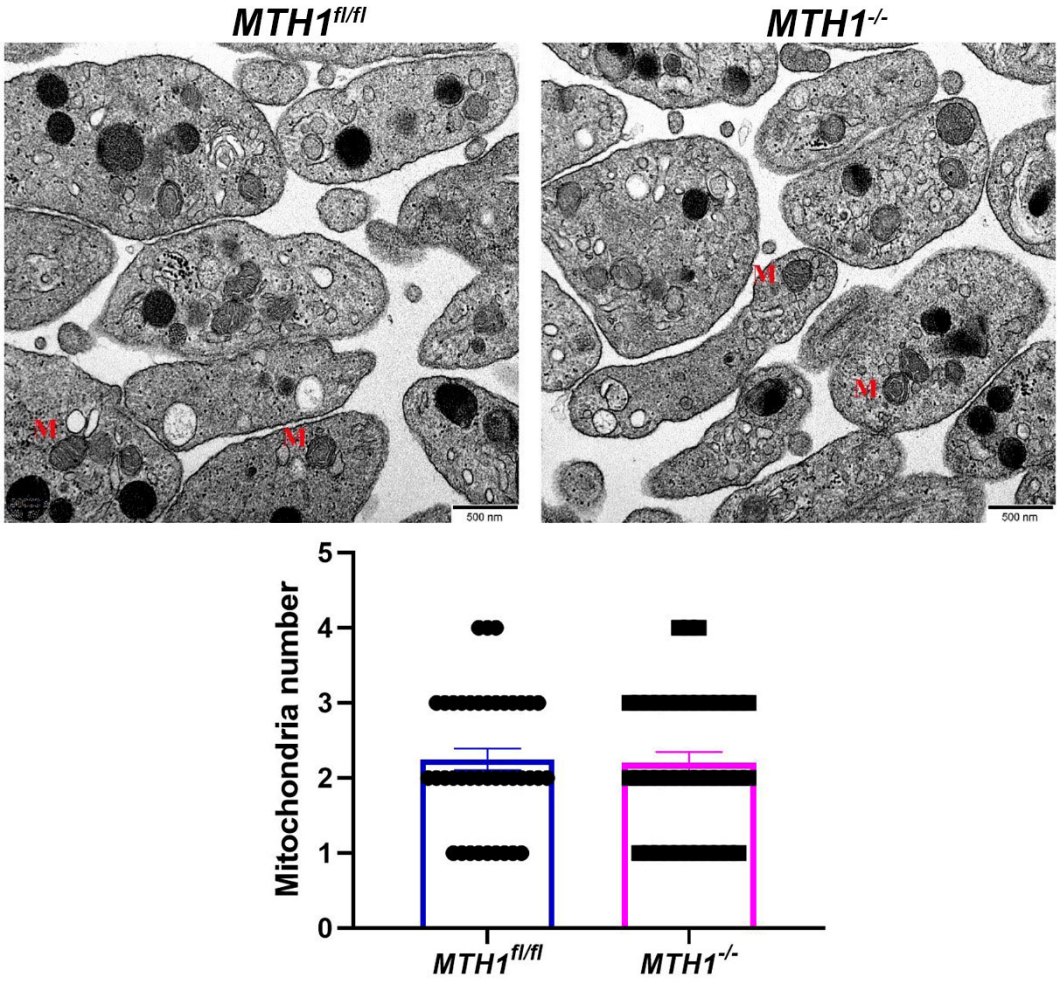


**Figure S11. Electron microscopic analysis of platelet mitochondria.** *MTH1*$^{fl/fl}$ or *MTH1*$^{-/-}$ platelets were fixed, dehydrated and embedded into an ultrathin section. After staining with lead citrate and uranyl acetate, mitochondria (indicated by M) was observed under a transmission electron microscope (x 30,000 magnification). Mitochondria numbers were counted in 40 platelets (mean ± SEM, n = 40, two-tailed Mann-Whitney test, $p = 0.8236$).

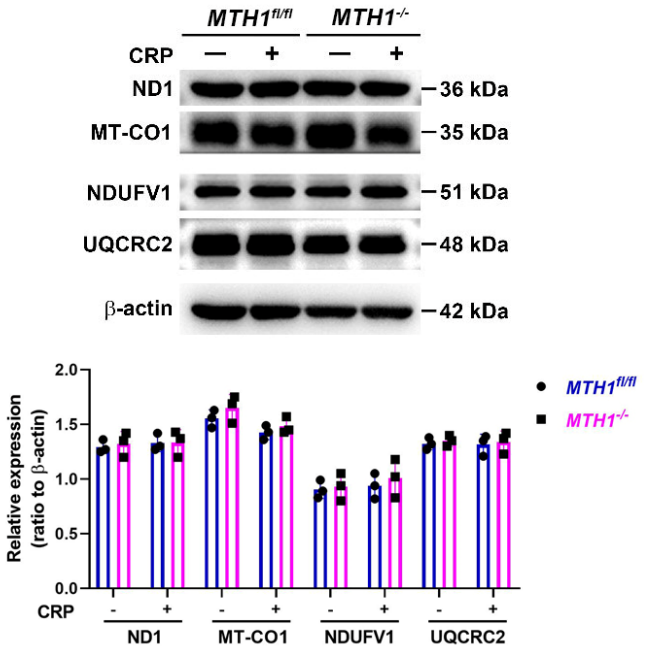


**Figure S12. Expression of proteins encoded by mitochondrial DNA or nuclear DNA.** Platelets were isolated from *MTH1*$^{fl/fl}$ or *MTH1*$^{-/-}$ mice and treated without (-) or with (+) CRP (5 μg/ml) for 3 mins followed by measuring the expression of ND1 ($p$ = 0.9999; $p$ = 0.9999), MT-CO1 ($p$ = 0.8928; $p$ = 0.9955), NDUFV1 ($p$ = 0.9999; $p$ = 0.9764), and UQCRC2 ($p$ = 0.9999; $p$ = 0.9999) (representative of three independent experiments) (mean ± SD, n = 3, two-way ANOVA with Sidak multiple comparisons test).

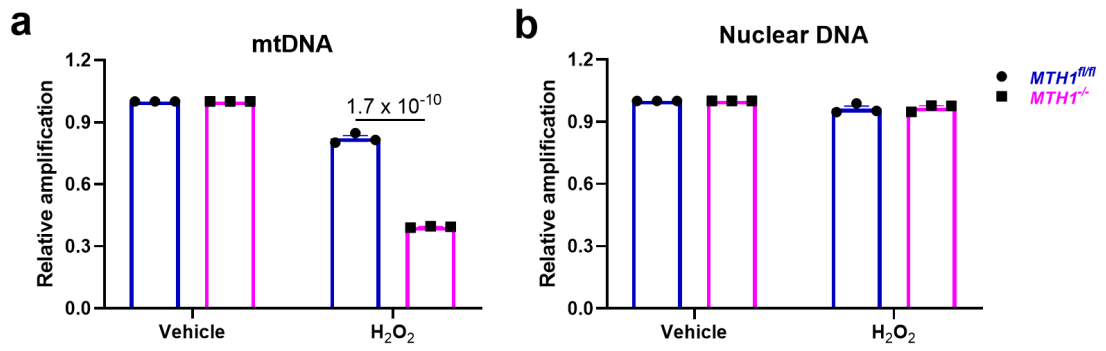


**Figure S13. Assessment of oxidative damage of mitochondrial DNA and nuclear DNA.** CD117$^{+}$ hematopoietic stem cells were isolated from *MTH1*$^{fl/fl}$ or *MTH1*$^{-/-}$ mice and cultured in vitro to induce their differentiation into megakaryocytes. Then, the collected megakaryocytes were treated with $H_2O_2$ (50 μM) for 30 min at room temperature to induce oxidative damage followed by isolation of total DNA to measure mitochondrial DNA damage ($p$ = 0.9999 for vehicle) **(a)** and nuclear DNA damage ($p$ = 0.9999 for vehicle; $p$ = 0.8906 for $H_2O_2$) **(b)** by quantitative PCR. The relative amplification was defined as a ratio relative to the vehicle treatment. Data were shown as mean ± SEM (n=3) and assessed by two-way ANOVA.

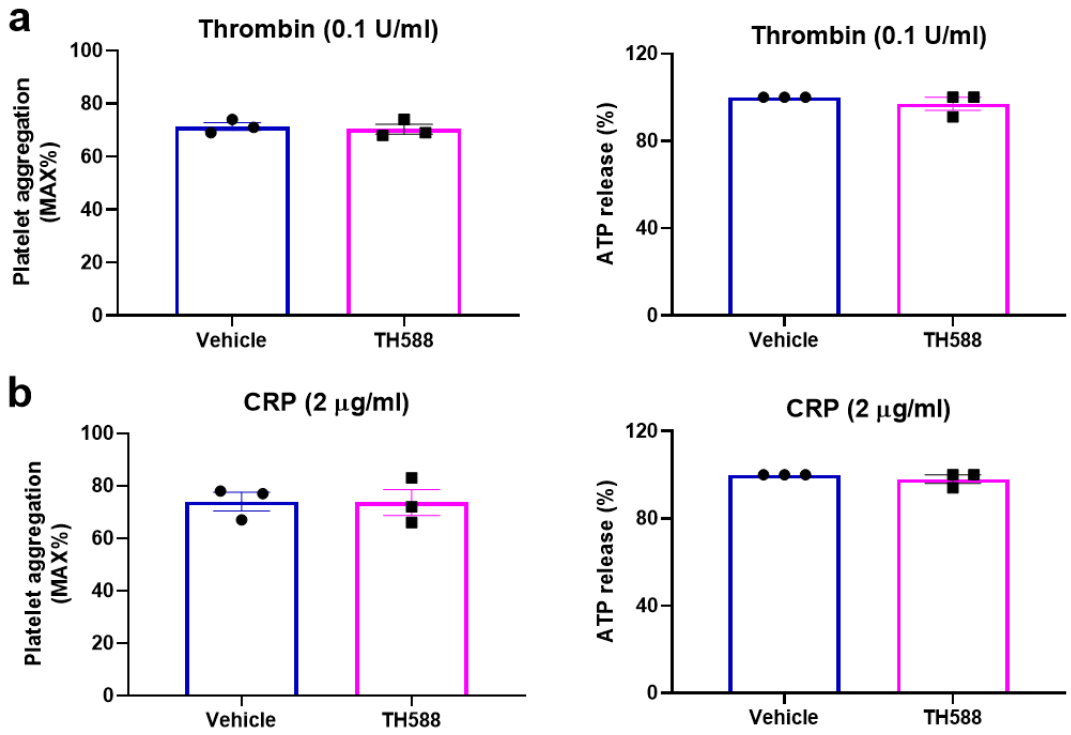


**Figure S14. Platelet aggregation and ATP release in human platelets.** Washed human platelets were pre-treated with 5 μM TH588 (MTH1 inhibitor) for 1 h at 37 °C followed by measuring platelet aggregation and ATP release in response to thrombin (0.1 U/ml) (mean ± SD, n = 3, two-tailed unpaired student's t-test) ($p$ = 0.6932; $p$ = 0.3739) **(a)** or CRP (2 μg/ml) (mean ± SD, n = 3, two-tailed unpaired student's t-test) ($p$ = 0.9590; $p$ = 0.3739) **(b)**.

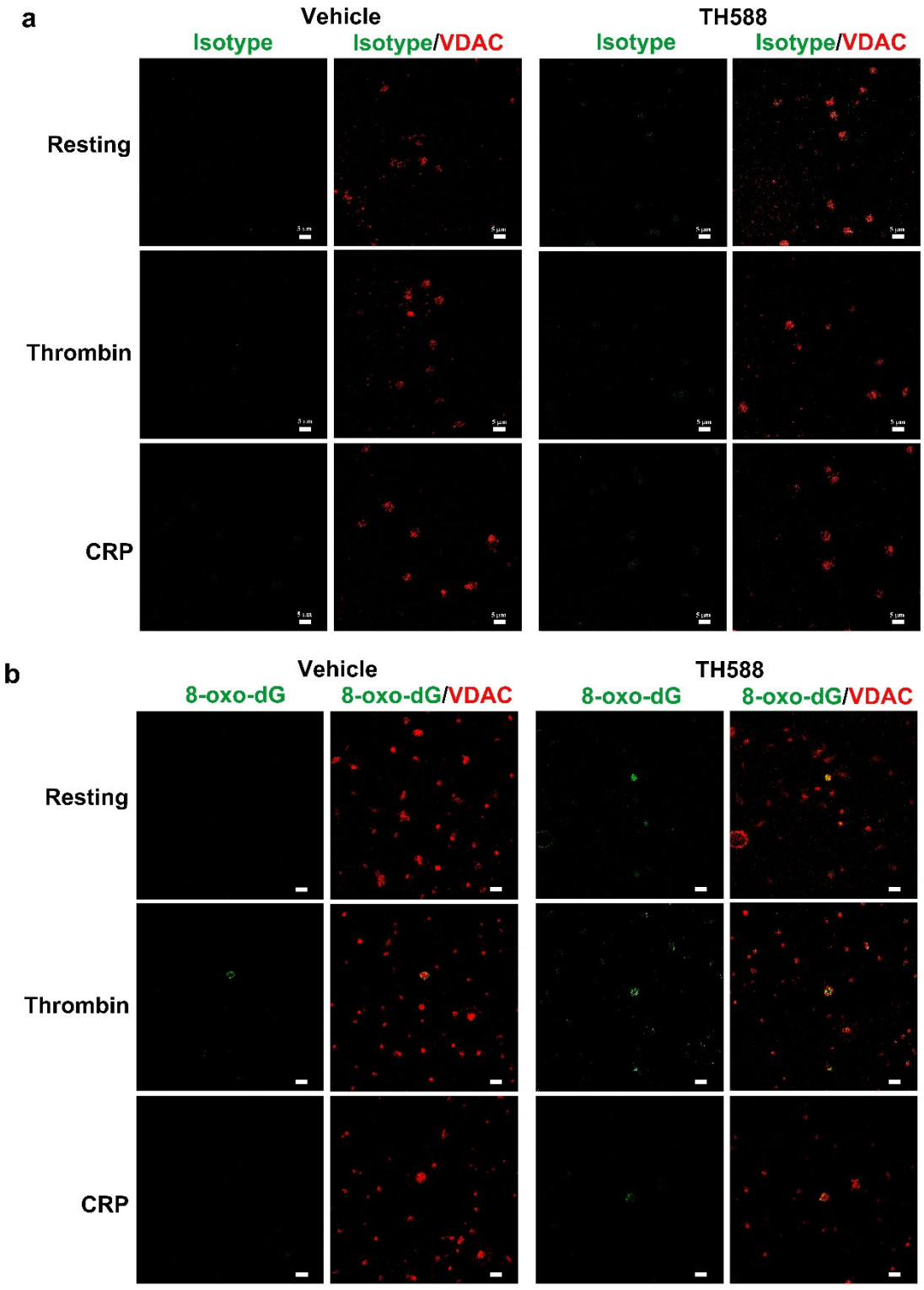


**Figure S15. Accumulation of 8-OHdG in mitochondria.** After TH588 treatment, human platelets were fixed, permeabilized and incubated with isotype control antibody IgG **(a)**, VDAC or 8-OHdG antibody **(b)** and then with fluorescence-labelled secondary antibodies. Platelets were mounted and staining was visualized under a confocal

microscopy. Representative images were shown from three independent experiments.

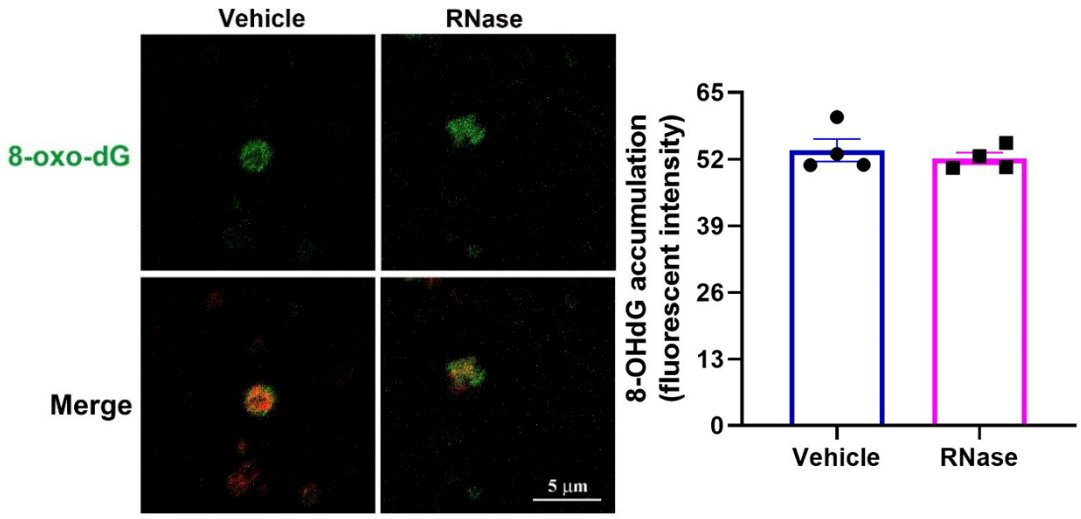


**Figure S16. 8-oxo-dG staining in human platelets.** Human platelets were pre-treated with 5 µM TH588 for 1 h at 37 °C and then stimulated with thrombin (1 U/ml) for 3 min followed by treatment with RNase A (0.02 mg/ml) for 30 minutes at 37°C. After that, platelets were stained with antibodies against with 8-oxo-dG or VDAC and then with secondary antibodies followed by observation of the staining under a confocal microscopy. Representative results from four independent experiments were shown (mean ± SEM, n=4, two-tailed unpaired student's t-test).

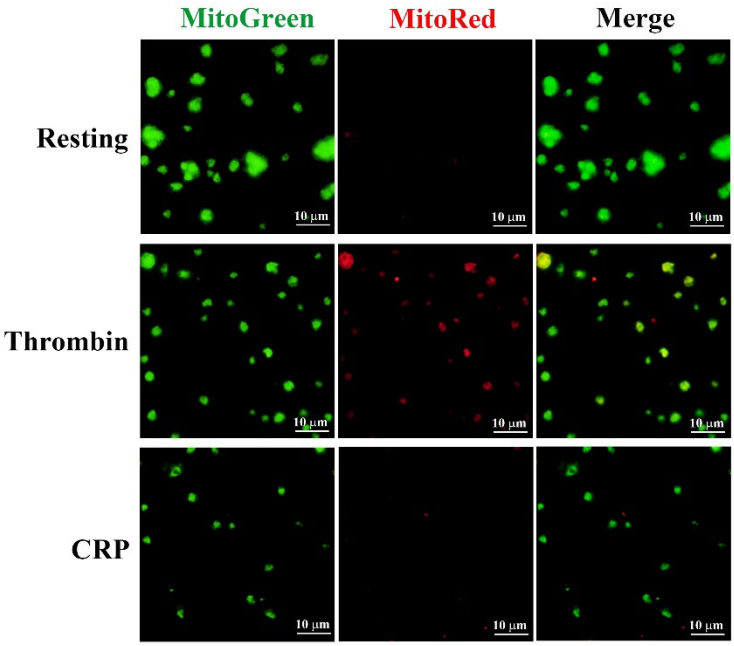


**Figure S17.** Mitochondrial ROS generation in human platelets. Platelets were preloaded with MitoSOX Red (5 μM) and MitoTracker Green (100 nM) for 10 min and then stimulated with thrombin (1 U/ml) or CRP (5 μg/ml) for 3 min to measured mitochondrial ROS generation by fluorescent microscope (x 100) (representative of three independent experiments).

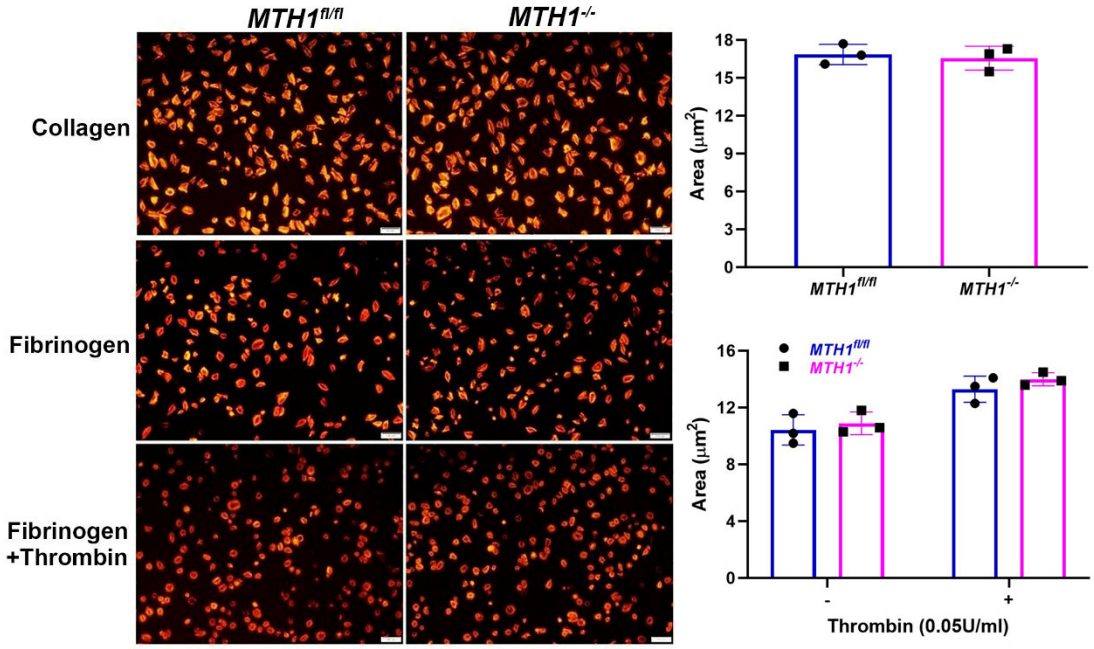


**Figure S18. Platelet spreading.** Platelets were placed on glass coverslips which were pre-coated with collagen or fibrinogen and then stained with Alexa Fluor-546-labelled phalloidin followed by observation under a microscope (X100) (scale bar = 20 μm) (mean ± SD, n = 3) (two-tailed unpaired student's t-test) ($p$ = 0.6966 for collagen; $p$ = 0.5766 for fibrinogen; $p$ = 0.3022 for fibrinogen + thrombin).

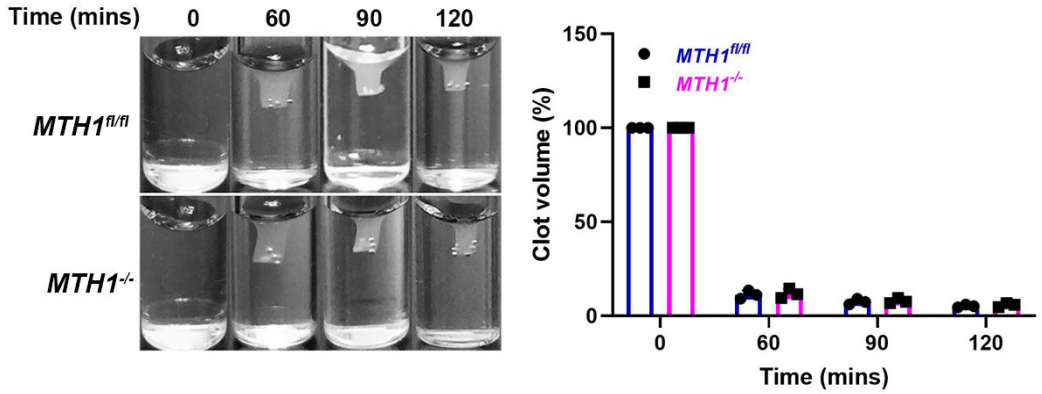


**Figure S19. Clot retraction.** Clot retraction was initiated after addition of thrombin (1 U/ml). Representative images at 60, 90 and 120 min. Data were quantified as clot volume (%) and presented as mean ± SD (n = 3) (Two-way ANOVA) ($p$ = 0.9999; $p$ = 0.9864; $p$ = 0.9980; $p$ = 0.9859).

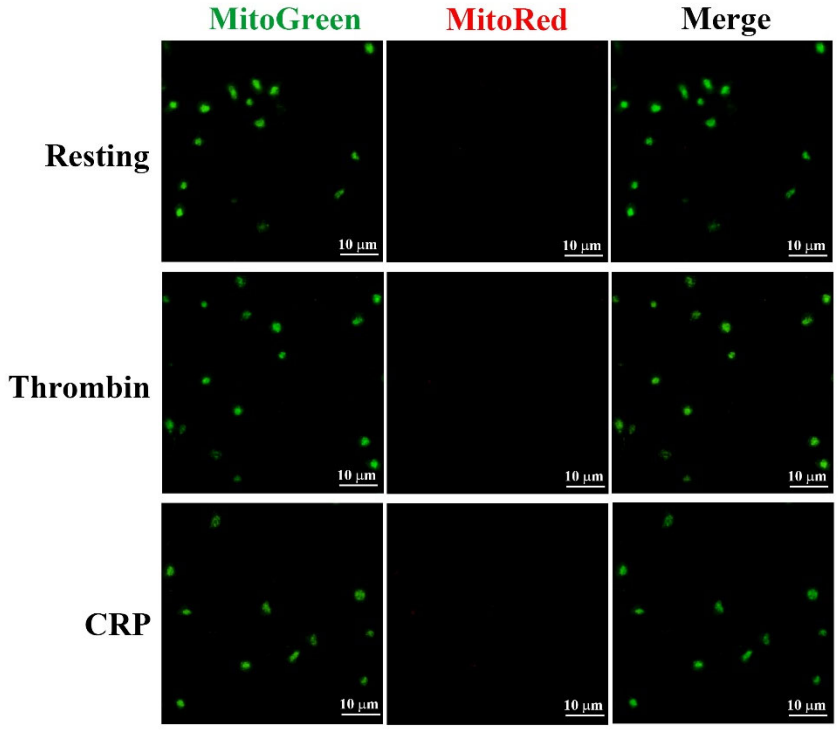


**Figure S20. Mitochondrial ROS production in mouse platelets.** After incubation with MitoSOX Red (5 μM) and MitoTracker Green (100 nM) for 10 min, platelets were treated with thrombin (1 U/ml) or CRP (5 μg/ml) for 1 min followed by analysis of mitochondrial ROS generation under a fluorescent microscope (x 100) (representative of three independent experiments).

**Supplementary Table**

**Table S1. Differentially expressed phosphopeptides between control and MTH1-deficient platelets after thrombin stimulation.**

| Protein Names | Gene Names | Modifications in Proteins | M-B /N-B | t test p value |
|---|---|---|---|---|
| C5a anaphylatoxin chemotactic receptor 1 | C5ar1 | S328 | 0.513488 | 0.047928 |
| Mitogen-activated protein kinase kinase kinase 3 | Map3k3 | S250 | 0.632597 | 0.034062 |
| Myeloid leukemia factor 2 | Mlf2 | Phospho [S] | 0.655886 | 0.019722 |
| Store-operated calcium entry-associated regulatory factor | Saraf | S326 | 0.711415 | 0.046403 |
| SRA stem-loop-interacting RNA-binding protein, mitochondrial | Slirp | S105 | 0.724269 | 0.003422 |
| Pleckstrin homology domain-containing family G member 2 | Plekhg2 | S1277 | 0.72478 | 0.040164 |
| Eukaryotic translation initiation factor 3 subunit D | Eif3d | S160 | 0.731345 | 0.022153 |
| Protein EVI2B | Evi2b | S264 | 0.732075 | 0.030371 |
| Endonuclease domain-containing 1 protein | Endod1 | S498 | 0.732556 | 0.019086 |
| Solute carrier family 22 member 23 | Slc22a23 | S12 | 0.742086 | 0.041613 |
| Protein LSM14 homolog A | Lsm14a | S183 | 0.756182 | 0.011512 |
| Ribosomal protein S6 kinase delta-1 | Rps6kc1 | Phospho [S] | 0.78095 | 0.037537 |
| Tricarboxylate transport protein, mitochondrial | Slc25a1 | S157 | 0.796303 | 0.021134 |
| Calmodulin-regulated spectrin-associated protein 1 | Camsap1 | S553 | 0.800323 | 0.035839 |
| T-complex protein 1 subunit zeta | Cct6a | S246 | 0.808225 | 0.021019 |
| Phostensin | Ppp1r18 | S194 | 0.823012 | 0.048407 |
| Phosphatidate cytidylyltransferase 2 | Cds2 | S59 | 1.203429 | 0.034157 |
| Krev interaction trapped protein 1 | Krit1 | T151 | 1.224572 | 0.0246 |
| Ras-related protein Rab-36 | Rab36 | S235 | 1.233705 | 0.015469 |
| A-kinase anchor protein 10, mitochondrial | Akap10 | S280 | 1.236161 | 0.011684 |
| B-cell lymphoma/leukemia 10 | Bcl10 | S138 | 1.269998 | 0.02903 |
| Ski oncogene | Ski | S429 | 1.412601 | 0.011619 |
| cAMP-specific 3',5'-cyclic phosphodiesterase 4A | Pde4a | S152(100) | 1.418573 | 0.009572 |

Data from 3 independent experiments were analyzed by two-tailed unpaired student's t-test.